Additional Supporting Information for "Sensitivity of warm clouds to large particles in measured marine aerosol size distributions – a theoretical study"

Tom Dror[1,*], J. Michel Flores[1,*], Orit Altaratz[1], Guy Dagan[2], Zev Levin[3], Assaf Vardi[4], and Ilan Koren[1]

[1]Department of Earth and Planetary Sciences, Weizmann Institute of Science, Rehovot, Israel.
[2]Atmospheric, Oceanic and Planetary Physics, Department of Physics, University of Oxford, Oxford, UK.
[3]School of Earth Sciences, Department of Geophysics, Tel Aviv University, Ramat Aviv, Israel.
[4]Department of Plant and Environmental Sciences, Weizmann Institute of Science, Rehovot, Israel.
[*]Contributed equally to this work.

Correspondence: Ilan Koren (ilan.koren@weizmann.ac.il)

Contents of this file

1. Figures S1 to S6

Introduction

Here we show all of the marine aerosol size distributions (MSDs) that were used as inputs to the model (Fig. S1), and the outputs of the model (i.e., rain yield and cloud's maximum mass) for the two shallower profiles used (Fig. S2). In addition, to gain a better understanding of the non-monotonic behavior of the surface rain yield and cloud's maximum total mass as a function of total aerosol concentration, we examined the time evolution of condensation–evaporation, collision–coalescence, and surface rain for the *Pacific-6* MSD (which does not contain giant or ultragiant particles; Fig. S3). We also show, that the *Atlantic-1* MSD has no optimal aerosol concentration (N_{op}) by running the model with aerosol concentrations of up to $10^6\,cm^{-3}$ (Fig. S4). Finally, we examine the time evolution of the total droplet surface area for all MSDs at four different total aerosol concentration (N_{tot}) concentrations (Fig. S5), and we investigate the droplet size distributions below cloud base for all MSDs for $N_{tot} = 2629\,cm^{-3}$ (Fig. S6).

Figure S1. Normalized MSDs

Six measured MSDs that represent a variety of different marine environments were normalized to the other five MSD concentrations (total of 36 MSDs). This allowed for a careful examination of the effect of both N_{tot} and the MSD's shape. Figure S1 presents all MSDs.

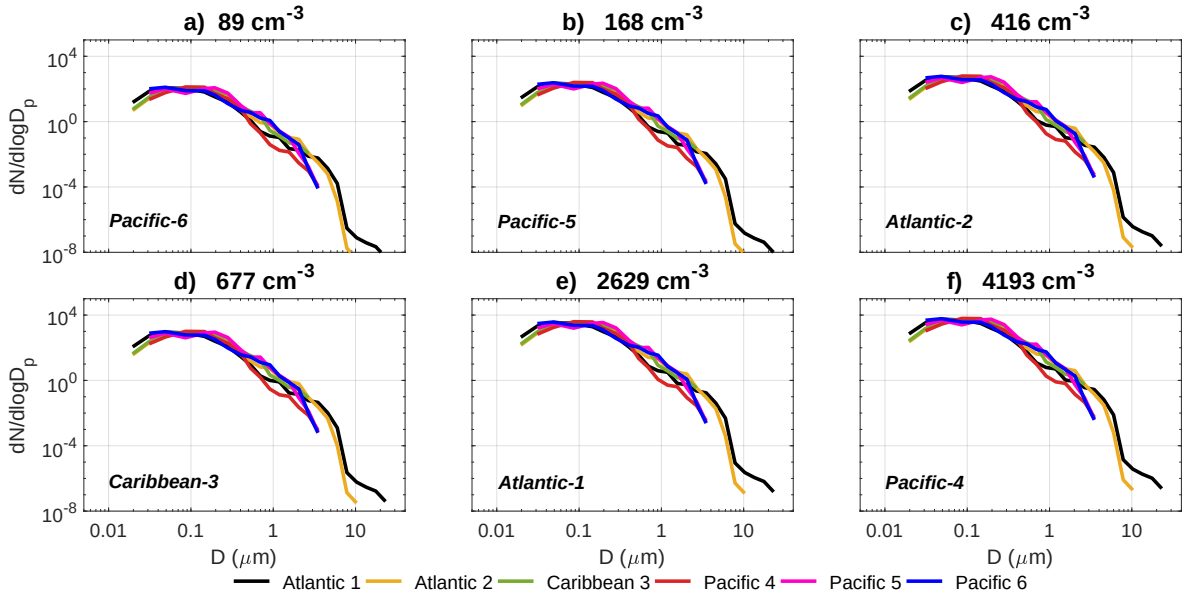

Figure 1. All of the MSDs used in the model. Each panel shows the MSDs normalized to the specific total aerosol concentration of the MSD noted in the lower left corner. The panels are organized from clean (a) to polluted (f) conditions.

Figure S2. Additional Atmospheric Profiles

To examine the effect of the different MSDs on cloud properties over a range of atmospheric conditions, we ran the model with three different sets of initial conditions. The initial conditions were based on idealized atmospheric profiles, describing a tropical moist environment (Garstang and Betts, 1974; Dagan et al., 2015). The three profiles are presented in Figure 1 of Dagan et al. (2015) and include: a well mixed sub-cloud layer between 0 and $\sim 1000\,m$ and a conditionally unstable cloudy layer between 1000 and, respectively, $4000\,m$, $3000\,m$, and $2000\,m$. The profiles were bounded by an overlying inversion layer with a temperature gradient of 2^oC over $50\,m$. Three different dewpoint temperatures were assigned to the profiles such that the relative humidity (RH) in the cloudy layer was 95%, 90%, and 80%, respectively. We examined the surface rain yield and the cloud's total maximum mass as a function of N_{tot}. The results from the deepest profile are shown in the main text (Fig. 2a,b), and the the other two profiles are shown in Figure S2. The behavior of surface rain yield and the cloud's total maximum mass as a function of N_{tot} strongly depends on the environmental conditions, i.e., the more unstable the profile (e.g., higher inversion height and RH in the cloudy layer), the more salient the revealed effect of the MSD. In all cases, the *Atlantic-1* clouds have a distinctively different behavior compared to the rest of the MSDs.

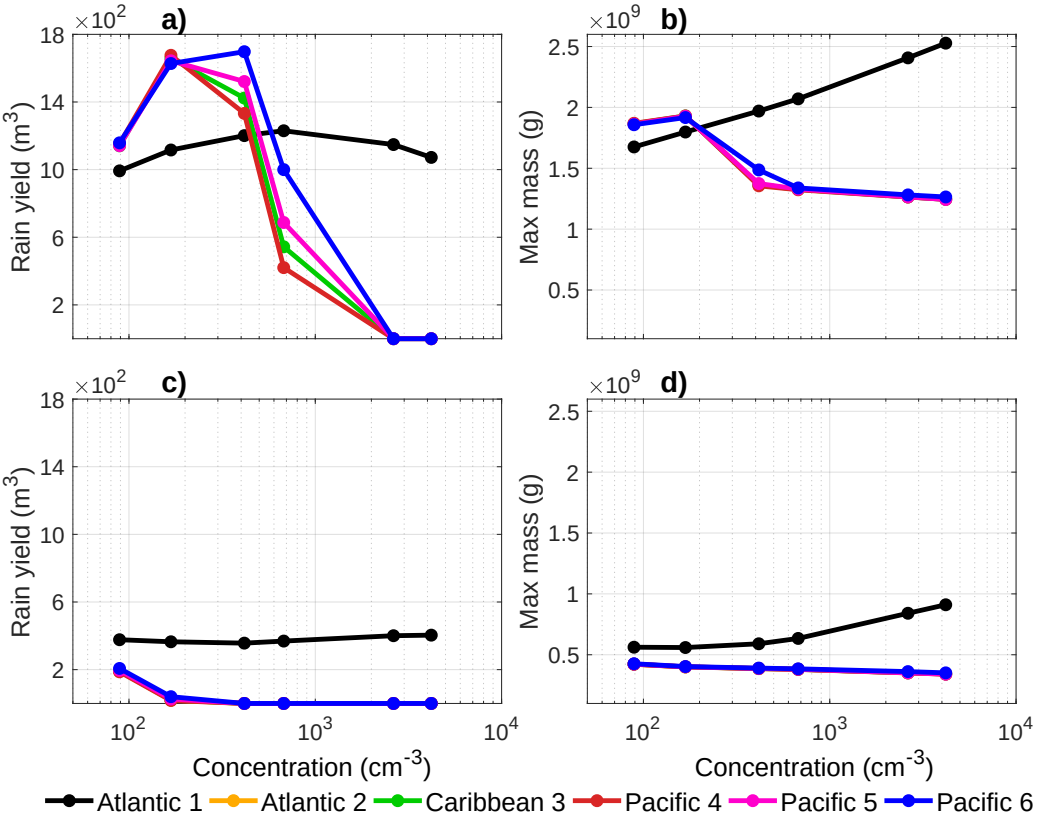

Figure 2. Surface rain yield (a and c) and cloud's maximum total mass (b and d) as a function of aerosol concentration for the two shallower profiles described in the main text. The top panels refer to an inversion height of $3000\,m$ and a RH of 90% in the cloudy layer. The lower panels refer to an inversion height of 2000 m with 80% RH in the cloudy layer. Each curve represents six simulations with a specific shape of the MSD normalized to a different aerosol concentration.

Figure S3. Cloud's Microphysical Processes

To understand the non-monotonic behavior of the surface rain yield and cloud's maximum total mass as a function of N_{tot}, we examined the time evolution of condensation–evaporation, collision-coalescence, and surface rain as the three major cloud processes. Figure S3 presents these processes for three different N_{tot} (clean, optimum and polluted conditions) using the *Pacific-6* MSD. The timing and the interaction between the processes are evident between the different clouds presented in Fig. S3. As N_{tot} increases (and the total droplet surface area becomes larger), so does the condensation efficiency (Pinsky et al., 2013; Seiki and Nakajima, 2014), and the collision–coalescence process is delayed. For the clean cloud, the early onset of collision–coalescence acts to further reduce the droplets' surface area, and triggers the early formation of rain. The more polluted the cloud is, the longer the time it has to grow by condensation (i.e., the peak in collision-coalescence drifts further away from the peak of condensation–evaporation). On the other hand, the delay in collision–coalescence allows entrainment processes to act for a longer time, resulting in enhanced evaporation. The cloud presented in Fig. S3b shows the evolution and

interaction of these processes under an optimal N_{tot} (N_{op}), for which the cloud mass (not shown) and surface rain yield are maximal. For the N_{op} scenario, the timing of the different cloud processes is ideal for cloud growth and rain-out (Dagan et al., 2015).

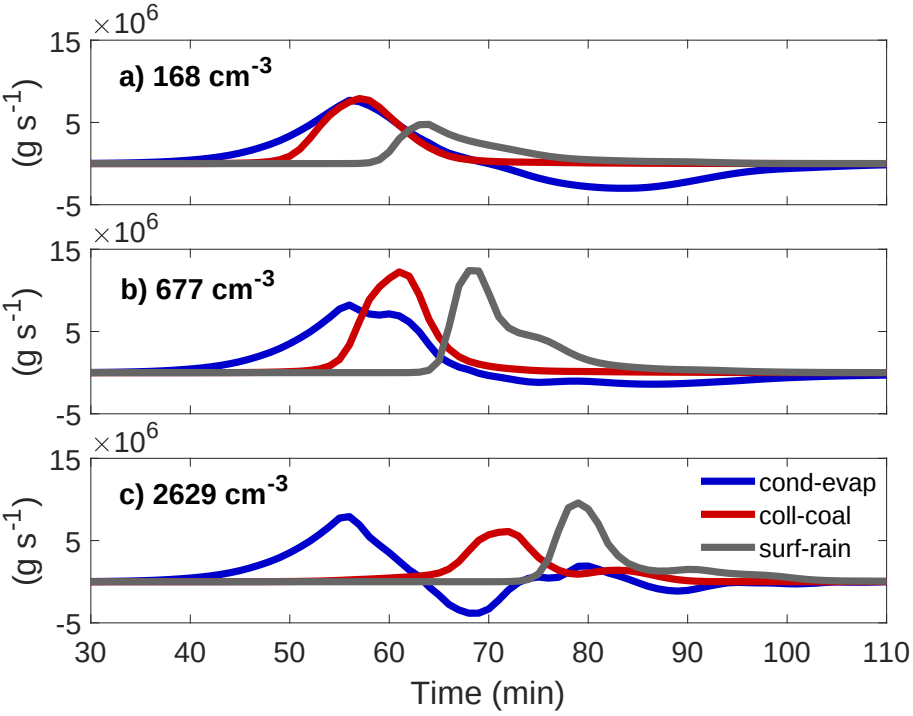

Figure 3. Total condensed–evaporated mass (blue), collected mass (red), and surface rain mass (gray) per unit time, as a function of time for the *Pacific-6* MSD for three different aerosol concentrations: clean (a), optimal (b), and polluted (c) for the deepest profile. The specific concentrations are noted on the upper left corner of each panel.

Figure S4. The *Atlantic-1* MSD Has No N_{op}

Additional sensitivity simulations were performed to examine the *Atlantic-1* MSD's behavior under extremely polluted conditions. Figure S4 shows the same as Figure 2a,b in the main text, but includes four additional simulations for the *Atlantic-1* MSD under N_{tot} of 10^4, 4×10^4, 10^5, and $10^6\, cm^{-3}$. From the figure, it is clear that a N_{op} does not exist for the *Atlantic-1* MSD.

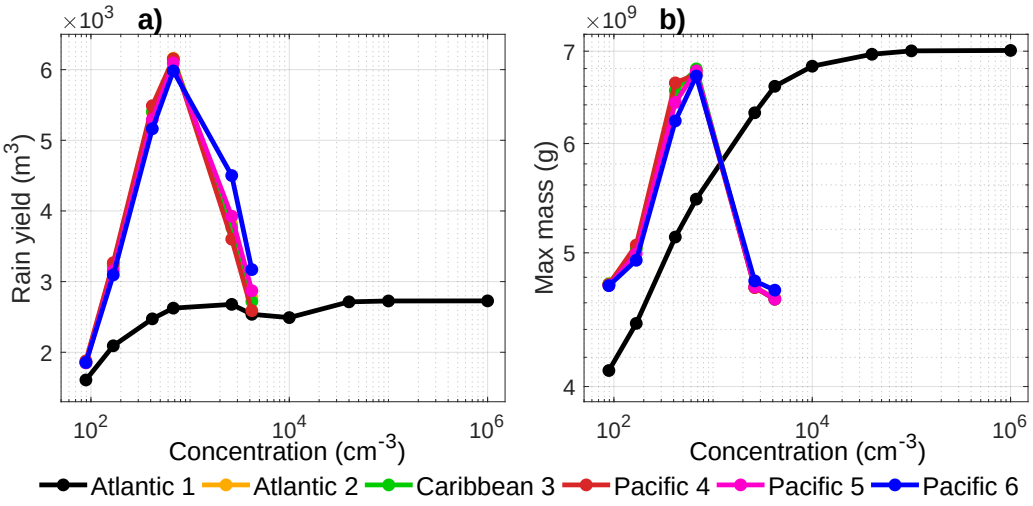

Figure 4. (a) Surface rain yield and (b) cloud's maximum total mass as a function of aerosol concentration used in the simulation. Each curve represents six simulations, performed with a specific shape of the MSD normalized to a different aerosol concentration, except for the *Atlantic-1* MSD that is comprised of 10 simulations up to an aerosol concentration of $10^6\,cm^{-3}$.

Figure S5. Total Droplet Surface Area Evolution

The temporal evolution of the total droplet surface area (summed over all cloudy pixels) was investigated for all MSDs, for four different aerosol concentrations (Fig. S5). The more polluted the clouds were (going from a to d in Fig. S5), the greater the difference in total droplet surface area between the *Atlantic-1* MSD and the rest of the MSDs. This is explained by the fact that the *Atlantic-1* MSD contains an ultragiant cloud condensation nuclei (UGCCN) mode, and as N_{tot} increased, the amount of UGCCN also increased (see Fig. 1), reducing the total droplet surface area.

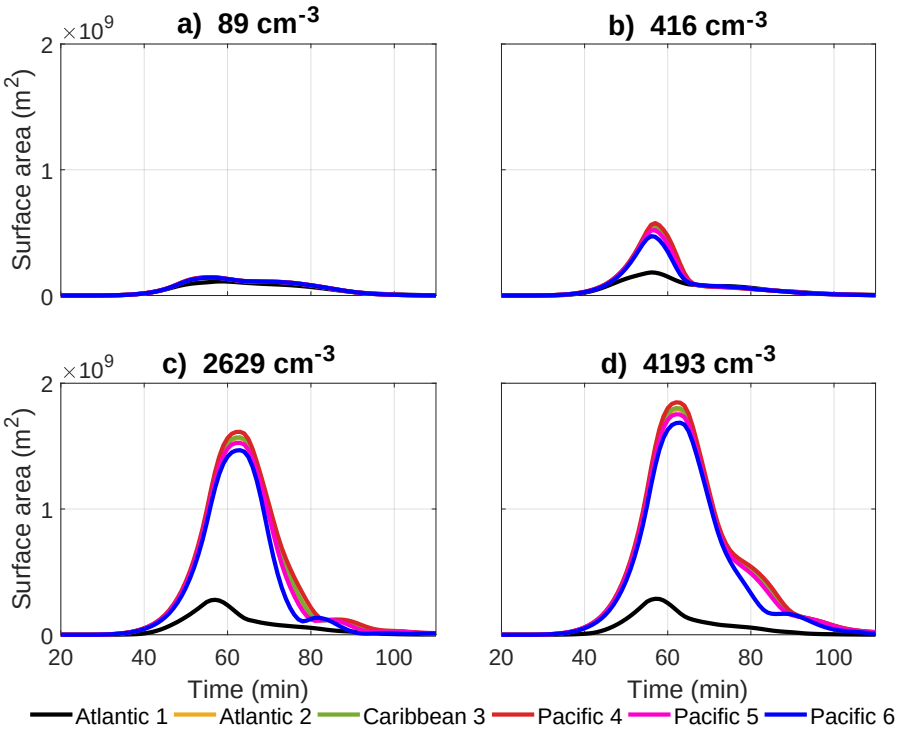

Figure 5. Total droplet surface area as for a total aerosol concentration of (a) $89\,cm^{-3}$, (b) $416\,cm^{-3}$, (c) $2629\,cm^{-3}$ and (d) $4193\,cm^{-3}$.

Figure S6. Droplet Size Distribution Below the Cloud Base

To understand the reduced surface rain caused by the enhanced evaporation below cloud base of the *Atlantic-1* MSD shown in Figure 3 of the main text, we calculated the mean droplet size distribution for the time of maximum rain for an area just below cloud base. Figure S6 shows the droplet size distribution for all of the MSDs for $N_{tot} = 2629\,cm^{-3}$. The biggest droplets in the *Atlantic-1* MSD case are seen to be about six orders of magnitude less in concentration compared to the other five MSDs, explaining the more efficient evaporation below cloud base.

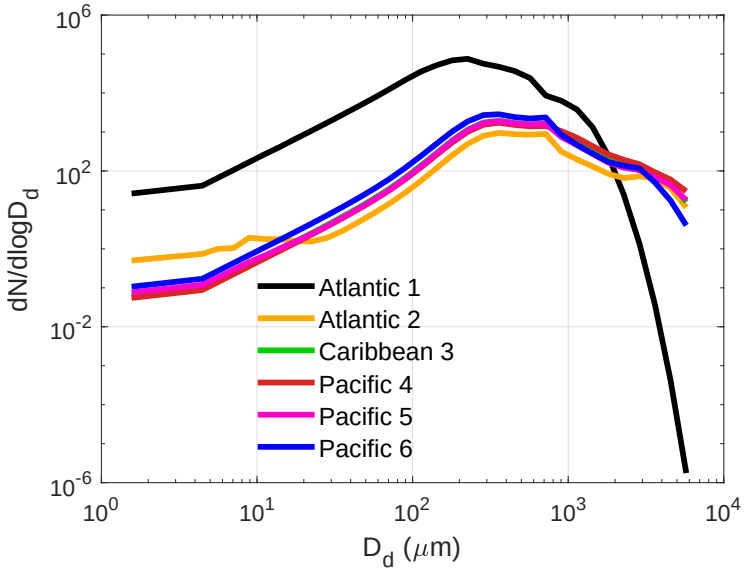

Figure 6. Droplet size distribution below cloud base at the time of maximum surface rain rate for the six different MSDs normalized to an aerosol concentration of $2629\,cm^{-3}$.

References

Dagan, G., Koren, I., and Altaratz, O.: Competition between core and periphery-based processes in warm convective clouds–from invigoration to suppression, Atmospheric Chemistry and Physics, 15, 2749–2760, 2015.

Garstang, M. and Betts, A. K.: A review of the tropical boundary layer and cumulus convection: Structure, parameterization, and modeling, Bulletin of the American Meteorological Society, 55, 1195–1205, 1974.

Pinsky, M., Mazin, I., Korolev, A., and Khain, A.: Supersaturation and diffusional droplet growth in liquid clouds, Journal of the Atmospheric Sciences, 70, 2778–2793, 2013.

Seiki, T. and Nakajima, T.: Aerosol effects of the condensation process on a convective cloud simulation, Journal of the Atmospheric Sciences, 71, 833–853, 2014.